J For Res (2013) 18:31–40
DOI 10.1007/s10310-012-0369-7

SPECIAL FEATURE: ORIGINAL ARTICLE

Lessons learned from CarboEastAsia: Carbon and water cycles in East Asian terrestrial ecosystems

Evaluation and improvement of MODIS gross primary productivity in typical forest ecosystems of East Asia based on eddy covariance measurements

Mingzhu He · Yanlian Zhou · Weimin Ju · Jingming Chen · Li Zhang · Shaoqiang Wang · Nobuko Saigusa · Ryuichi Hirata · Shohei Murayama · Yibo Liu

Received: 28 December 2011 / Accepted: 14 July 2012 / Published online: 24 October 2012

Abstract Gross primary productivity (GPP) is a major component of carbon exchange between the atmosphere and terrestrial ecosystems and a key component of the terrestrial carbon cycle. Because of the large spatial heterogeneity and temporal dynamics of ecosystems, it is a challenge to estimate GPP accurately at global or regional scales. The 8-day MODerate resolution Imaging Spectroradiometer (MODIS) GPP product provides a near real time estimate of global GPP. However, previous studies indicated that MODIS GPP has large uncertainties, partly caused by biases in parameterization and forcing data. In this study, MODIS GPP was validated using GPP derived from the eddy covariance flux measurements at five typical forest sites in East Asia. The validation indicated that MODIS GPP was seriously underestimated in these forest ecosystems of East Asia, especially at northern sites. With observed meteorological data, fraction of photosynthetically active radiation absorbed by the plant canopy (fPAR) calculated using smoothed MODIS leaf area index, and optimized maximum light use efficiency (ε_{max}) to force the MOD17 algorithm, the agreement between predicted GPP and tower-based GPP was significantly improved. The errors of MODIS GPP in these forest ecosystems of East Asia were mainly caused by uncertainties in ε_{max}, followed by those in fPAR and meteorological data. The separation of canopy into sunlit and shaded leaves, for which GPP is individually calculated, can improve GPP simulation significantly.

Keywords Forest ecosystem · Gross primary productivity · Maximum light use efficiency · MODIS GPP · Sunlit/shaded leaves

Introduction

The terrestrial carbon cycle is an important component of the global carbon cycle. It is crucial for reliably predicting

Electronic supplementary material The online version of this article (doi:10.1007/s10310-012-0369-7) contains supplementary material, which is available to authorized users.

M. He · W. Ju (✉) · J. Chen · Y. Liu
Jiangsu Provincial Key Laboratory of Geographic Information Science and Technology, International Institute for Earth System Science, Nanjing University, 901 Mengminwei Building, 22 Hankou Road, Nanjing 210093, China
e-mail: juweimin@nju.edu.cn

Y. Zhou
School of Geographic and Oceanographic Sciences, Nanjing University, Nanjing 210093, China

L. Zhang
Key Laboratory of Ecosystem Network Observation and Modeling, Institute of Geographic Sciences and Natural Resources Research, Chinese Academy of Sciences, Beijing 100101, China

S. Wang
Qianyanzhou Ecological Experimental Station, Institute of Geographic Sciences and Natural Resources Research, Chinese Academy of Sciences, Beijing 100101, China

N. Saigusa · R. Hirata
Center for Global Environmental Research, National Institute for Environmental Studies, 16-2 Onogawa, Tsukuba 305-8506, Japan

S. Murayama
Research Institute for Environmental Management Technology, National Institute of Advanced Industrial Science and Technology (AIST), AIST Tsukuba West, 16-1 Onogawa, Tsukuba 305-8569, Japan

future atmospheric carbon dioxide (CO_2) concentration and climate changes and for understanding the interactions between the atmosphere and biosphere (Li et al. 2008). Gross primary productivity (GPP) of terrestrial ecosystems is a critical component of the terrestrial carbon cycle (Yang et al. 2007). It is an indicator for quantitatively describing the productivity of ecosystems. Quantitative estimates of the spatial and temporal distribution of GPP at regional or global scales are important for understanding the response of ecosystems to increases in atmospheric CO_2 and temperature and are thus central to policy-relevant decisions (Metz et al. 2006).

It is a challenge to estimate regional/global GPP reliably. Recently, remote sensing has been used as an effective tool for estimating GPP for the global land surface. Since February 2000, data from the MODerate resolution Imaging Spectroradiometer (MODIS) has been used to provide global GPP at a resolution of 1 km and an 8-day interval, which is known as MOD17 in the MODIS land products (Zhao and Running 2006). The method for calculating MODIS GPP is the MOD17 algorithm, which calculates GPP as the product of absorbed photosynthetically active radiation (APAR), prescribed maximum light use efficiency (ε_{max}) for each land cover type, and scalars of temperature and vapor pressure deficit (VPD). APAR is calculated as the product of incoming photosynthetically active radiation (PAR) and the fraction of photosynthetic active radiation (fPAR) estimated from remote sensing data. Many validations show that MODIS GPP has some errors (Baldocchi et al. 2001; Turner et al. 2003, 2005; Leuning et al. 2005; Zhao et al. 2005; Zhao and Running 2006; Nightingale et al. 2007; Zhang et al. 2008).

The errors of MODIS GPP are partly caused by uncertainties in input data. Zhao et al. (2005) pointed out that the underestimation of VPD may lead to the overestimation of GPP, and the largest uncertainties in GPP exist in the tropical regions. The underestimation of VPD interpolated from the Data Assimilation Office (DAO) meteorological data and exclusion of soil moisture effects in the MOD17 algorithm could be responsible for the errors of MODIS GPP across the United States (Baldocchi et al. 2001; Turner et al. 2003; Heinsch et al. 2006). Nightingale et al. (2007) declared that MODIS GPP might be consistently overestimated in drought regions. Leuning et al. (2005) confirmed that errors in APAR could be the major explainer for the errors in MODIS GPP. In the MOD17 algorithm, fPAR is calculated from MODIS leaf area index (LAI), which might have some uncertainties. Running et al. (2004) indicated that MODIS LAI tends to be overestimated at a coniferous forest site in Finland. Hill et al. (2006) pointed out that MODIS LAI is quite poor in some coastal and highland forests in Eastern and Western Australia due to clouds and poor retrieval of reflectance. It was generally overestimated in dry and wet seasons in a tropical savanna in the Northern Territory of Australia (Kanniah et al. 2009). Zhang et al. (2008) found that MOD17 GPP was underestimated in typical cropland and alpine meadow ecosystems in China, partly owing to the underestimation of MODIS LAI. Maximum light use efficiency (ε_{max}) is a key parameter for MODIS GPP calculation and assigned according to land cover types. Zhang et al. (2008) indicated that the underestimation of ε_{max} is the main reason for the considerable underestimation of GPP calculated using the MOD17 algorithm in two biomes in China, especially at a cropland site. Running et al. (2004) pointed out that the most significant limitation of the MOD17 algorithm is the improper parameterization of light use efficiency.

In the MOD17 algorithm, GPP is calculated by treating the whole canopy as a big leaf. However, many studies have indicated that the big-leaf method would induce large errors in modeled results because the quantum response of leaf photosynthesis is non-linear and the photosynthetic active radiation (PAR) intercepted by the sunlit leaves in the canopy is significantly different from that intercepted by shaded leaves (Wang and Leuning 1998; Chen et al. 1999). Shaded leaves can receive only diffused PAR and their photosynthesis is mostly limited by low PAR. In contrast, sunlit leaves can intercept both direct and diffused PAR and their photosynthesis is often PAR saturated. It is now generally realized that PAR intercepted by the canopy must be separated into direct and diffused components for better calculation of canopy GPP since diffused PAR would have greater light use efficiency than direct PAR. Shaded leaves would intercept greater PAR per leaf area and have increased photosynthesis rates with the increase of diffused PAR (Gu et al. 2002; Oliphant et al. 2011). Studies have demonstrated that two-leaf models perform better than big-leaf models in calculating canopy carbon sequestration by separating the canopy into sunlit and shaded leaves, for which GPP is calculated individually (Norman 1993; De Pury and Farquhar 1997; Wang and Leuning 1998; Chen et al. 1999).

The main objectives of this study are: (1) to evaluate the MOD17 GPP product at five typical forest ecosystems in East Asia using tower-based GPP, and (2) to identify the possible way to improve GPP calculated using the MOD17 algorithm and MODIS LAI data.

Method and data

Method

To fulfill the goals of this study, the MODIS GPP was first validated using tower-based GPP, which we refer to as GPP_FLUX hereafter. Then, locally measured

meteorological data, fPAR calculated using smoothed MODIS LAI, and calibrated ε_{max} were individually or simultaneously used to drive the MOD17 algorithm. Calculated GPP was compared with GPP_FLUX to identify the possible causes of errors in MODIS GPP. Finally, the ability of a new algorithm to improve GPP estimation was also investigated, one which separates the canopy into sunlit and shaded leaf groups to calculate GPP using the MOD17 algorithm.

Data

GPP_FLUX used to evaluate simulated GPP was derived from net ecosystem exchange (NEE) measured at five typical forest ecosystems in East Asia, including Changbai Mountain pine and broadleaf mixed forest site (CBS) (Yu et al. 2006; Zhang et al. 2006a), Qianyanzhou planted coniferous forest site (QYZ) (Yu et al. 2006; Zhang et al. 2006b), Dinghushan South Subtropical evergreen broadleaved forest site (DHS) (Yu et al. 2006; Zhang et al. 2006b), Tomakomai Japanese larch forest site (TMK) (Hirata et al. 2007), and Takayama deciduous broadleaf forest site (TKY) (Saigusa et al. 2005). Site characteristics of these flux towers are listed in Table S1. Half-hourly GPP was calculated from half-hourly measured NEE using the method of Chinaflux (Fu et al. 2006; Yu et al. 2006) and summed to 8-day totals. Meteorological data measured every 30 min at the tower sites, including PAR, air temperature (T_a), and VPD, were averaged or summed to produce daily values to force the MOD 17 algorithm.

The 1 km 8-day MODIS GPP and LAI products used here were downloaded from the Land Processes-Distributed Active Archive Center (LPDAAC) (http://lpdacc.usgs.gov/). MODIS Reprojection Tools (MRT) was used to project MOD15 and MOD17 products into an UTM/WGS 84 projection. In order to remove residual cloud contamination, the annual time series of downloaded MODIS LAI was smoothed using the locally adjusted cubic-spline capping (LACC) method (Chen et al. 2006).

In order to assess the effects of parameter calibration and the sunlit and shaded leaf separation approach on simulated regional GPP, the daily reanalysis meteorological data in 2003 over the region of East Asia (17.00–60.00°N, 65.00–150.00°E) were downloaded from the US National Centers for Environmental Prediction (NCEP) and interpolated to a spatial resolution of 1 km to drive the MOD17 algorithm (Zhang et al. 2012).

The MOD17 algorithm

The MOD17 algorithm calculates GPP as the product of light use efficiency and APAR (Running et al. 2004). Parameterization of this algorithm was implemented following Sala et al. (2000). Light use efficiency is downscaled from the prescribed biome-specific ε_{max} with the consideration of the effects of minimum temperature and VPD on GPP. APAR is calculated from MODIS LAI (Heinsch et al. 2003; Zhang et al. 2008).

GPP calculated using a sunlit and shaded leaves separation approach

In order to consider differences in APAR and light use efficiency of sunlit and shaded leaves, canopy GPP is calculated as:

$$\begin{aligned}\mathrm{GPP} = {} & \varepsilon_{\mathrm{max\_sunlit}} f(\mathrm{VPD}) f(T_{\mathrm{a\,min}}) \mathrm{APAR}_{\mathrm{sun}} \\ & + \varepsilon_{\mathrm{max\_shaded}} f(\mathrm{VPD}) f(T_{\mathrm{a\,min}}) \mathrm{APAR}_{\mathrm{shaded}}\end{aligned} \quad (1)$$

where ε_{max_sunlit} and ε_{max_shaded} are the maximum light use efficiency of sunlit and shaded leaves and were calibrated using GPP_FLUX. $APAR_{sun}$ and $APAR_{shaded}$ are PAR absorbed by sunlit and shaded leaves and computed as:

$$\begin{aligned}\mathrm{APAR}_{\mathrm{sun}} = {} & [(1-\alpha)\mathrm{PAR}_{\mathrm{dir}} \cos(\beta)/\cos(\theta) \\ & + \mathrm{PAR}_{\mathrm{shaded}}]\mathrm{LAI}_{\mathrm{sunlit}}\end{aligned} \quad (2)$$

$$\begin{aligned}\mathrm{APAR}_{\mathrm{shaded}} = {} & (1-\alpha)[(\mathrm{PAR}_{\mathrm{dif}} - \mathrm{PAR}_{\mathrm{dif\_under}}) \\ & /\mathrm{LAI} + C]\mathrm{LAI}_{\mathrm{shaded}}\end{aligned} \quad (3)$$

where PAR_{dif} and PAR_{dir} are the direct and diffused components of incoming PAR, respectively; PAR_{dif_under} is the diffused PAR under the canopy; C denotes the multiple scattering of the direct PAR (Chen et al. 1999); α is the albedo of the canopy; LAI_{sunlit} and LAI_{shaded} are the sunlit and shaded leaf area index and determined according to total LAI, clumping index, and solar zenith angle (Chen et al. 1999).

PAR_{dir} equals total PAR minus PAR_{dif}, which was determined according to sky clearness index (Chen et al. 1999):

$$\mathrm{PAR}_{\mathrm{dif}} = \begin{cases} \mathrm{PAR}(0.7527 + 3.8453R - 16.316R^2 \\ \quad +18.962R^3 - 7.0802R^4) & R < 0.8 \\ 0.13\mathrm{PAR} & R \geq 0.8 \end{cases} \quad (4)$$

where PAR is the total incoming PAR, equal to 50 % of incoming solar radiation (S_g); R is the sky clearness index and calculated as:

$$R = S_g/(S_0 \cos\theta) \quad (5)$$

where S_0 is the solar constant (1367 W m^{-2}) and θ is the solar zenith angle.

Simulation experiments

Four site-level simulations were conducted in this study (Table 1). Simulation I was designed to assess the impact of uncertainties in meteorological data on GPP calculation,

Table 1 Description of four site-level and three regional-level simulations made in this study

	Meteorological data	fPAR	ε_{max}	Output
Site-level				
Simulation I	Observed meteorological data	Estimated from MODIS LAI	Default	GPP_REV1
Simulation II	Observed meteorological data	Estimated from smoothed MODIS LAI	Default	GPP_REV2
Simulation III	Observed meteorological data	Estimated from smoothed MODIS LAI	Optimum ε_{max}	GPP_REV3
Simulation IV	Observed meteorological data	Estimated from smoothed MODIS LAI for sunlit and shaded leaves	Optimum ε_{max} for sunlit and shaded leaves	GPP_REV4
Regional-level				
Simulation II	Interpolated NCEP data	Estimated from smoothed MODIS LAI	Default	GPP_R_S1
Simulation III	Interpolated NCEP data	Estimated from smoothed MODIS LAI	Optimum ε_{max}	GPP_R_S2
Simulation IV	Interpolated NCEP data	Estimated from smoothed MODIS LAI for sunlit and shaded leaves	Optimum ε_{max} for sunlit and shaded leaves	GPP_R_S3

and the resultant GPP was named as GPP_REV1. Simulation II was to investigate the effect of removing residual cloud contamination in MODIS LAI on GPP calculation, and the resultant GPP was named as GPP_REV2. Simulation III was designed to investigate the effect of ε_{max} parameterization on GPP calculation. The parameter ε_{max} was calibrated through maximizing the determination coefficient of GPP estimated using locally measured meteorological data and smoothed LAI. The resultant GPP was named as GPP_REV3. In simulation IV, the canopy was stratified into sunlit and shaded leaves, for each of them GPP was separately calculated using calibrated locally measured meteorological data, smoothed MODIS LAI, and calibrated ε_{max} of each leaf group. The goal of this simulation was to explore the possibility of improving GPP calculation using a sunlit and shaded leaf separation approach.

Similarly, three regional simulations were also conducted to investigate the effects of ε_{max} calibration using tower-measured GPP and the sunlit and shaded leaf separation approach on regional GPP calculations over East Asia (17.0–60.0°N, 65.0–150.0°E) (Table 1).

Results

Evaluation of MODIS GPP

Figure 1 shows MODIS GPP (GPP_MODIS) and GPP_FLUX at five study sites. They exhibited very similar seasonal variations. However, GPP_MODIS was lower than GPP_FLUX in the growing seasons at all sites. The underestimation of GPP_MODIS was more obvious at the CBS, TMK and TKY sites than at the QYZ and DHS sites.

At CBS, GPP_MODIS was systematically lower than GPP_FLUX in the growing seasons. In non-growing seasons, by late October, GPP_MODIS approached zero while GPP_FLUX remained at low values (Fig. 1a). The annual means of 8-day GPP_MODIS were underestimated by 72.2 and 70.6 % in 2003 and 2004, respectively. The R^2 values for the correlation between 8-day GPP_MODIS and GPP_FLUX were 0.91 and 0.96, and the corresponding RMSE values were 3.98 and 3.77 g C m^{-2} d^{-1} in these 2 years (Table S2).

At QYZ, GPP_MODIS showed similar seasonality, but larger fluctuations compared with GPP_FLUX. This site was hit by an abnormal high temperature and drought in the summer of 2003, causing carbon sequestration to decrease considerably from DOY 177 to 225 (Sun et al. 2006) (Fig. 1b). However, GPP_MODIS failed to respond to this climatic abnormality. The R^2 values of 8-day GPP_MODIS against GPP_FLUX were 0.72 and 0.67 in 2003 and 2004, respectively. The corresponding RMSE values were 1.99 and 2.51 g C m^{-2} d^{-1}. The annual means of GPP_MODIS were underestimated by 34.04 and 46.97 % in 2003 and 2004, respectively (Table S2).

At DHS, GPP_MODIS was slightly underestimated before summer and overestimated after summer in 2003. It was overestimated in winter and early spring and obviously underestimated in the period from late spring to autumn in 2004 (Fig. 1c). The agreement between GPP_MODIS and GPP_FLUX was quite poor, with the R^2 values of 0.37 and 0.19 and RMSE values of 2.12 and 1.70 g C m^{-2} d^{-1} in 2003 and 2004, respectively (Table S2). The annual means of GPP_MODIS were 6.08 and 16.52 % lower than those of GPP_FLUX in two study years.

At TMK, GPP_FLUX increased rapidly in early May, and peaked in early June and then declined gradually. In contrast, GPP_MODIS fluctuated marginally around 3.0 g C m^{-2} d^{-1} during this period (Fig. 1d). The annual means of GPP_MODIS were only 34.75–44.98 % of the GPP_FLUX values in years from 2001 to 2003. The R^2 values of 8-day GPP_MODIS against GPP_FLUX were 0.60, 0.62, 0.68, and the corresponding RMSE values were 4.49, 3.31, 4.80 g C m^{-2} d^{-1} in three study years (Table S2).

At TKY, MODIS_GPP increased much faster than GPP_FLUX in early spring and then remained

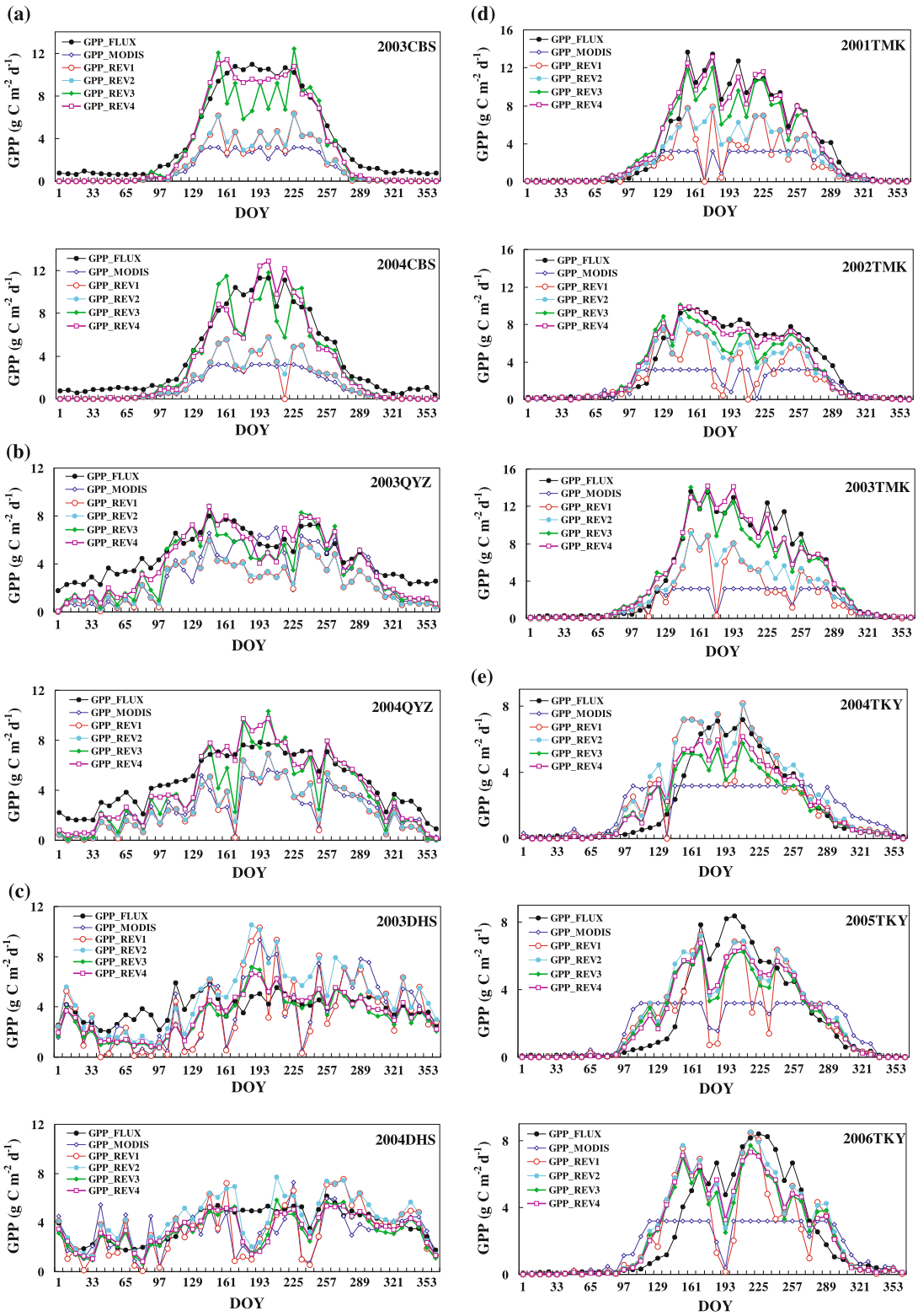

Fig. 1 Time series of 8-day estimated from EC (GPP_FLUX), 8-day MODIS GPP (MODIS GPP), 8-day GPP simulated using the MOD17 algorithm with the calibrated ε_{max} (GPP_MOD3), and 8-day GPP simulated by separation of sunlit and shaded leaves with the MOD17 algorithm (GPP_MOD4) at CBS (**a**), QYZ (**b**), DHS (**c**), TMK (**d**) and TKY (**e**) of East Asia

approximately at 3.0 g C m^{-2} d^{-1} in summer and early autumn. It started to decline later than GPP_FLUX in the middle of autumn. The annual means of 8-day GPP_MODIS were 11.5–30.5 % lower than the values of GPP_FLUX from 2004 to 2006. The R^2 values of GPP_MODIS against GPP_FLUX were 0.51, 0.41, and 0.50 and the RMSE values were 1.78, 2.19, 2.26 g C m^{-2} d^{-1} in three study years (Table S2).

GPP calculated using observed meteorological data

The application of measured meteorological data to drive the MOD17 algorithm obviously improved the agreement between simulated GPP and GPP_FLUX (Fig. 1; Table S2). The underestimation of GPP_MODIS in the growing seasons was significantly corrected at CBS, TMK and TKY. At QYZ, GPP_REV1 showed a noticeable decline similar to GPP_FLUX during the hot and drought period in the middle of summer of 2003. The improvement on calculated GPP through using observed meteorological data was more significant at CBS, TKY and TMK than at QYZ and DHS, indicating that the errors of GPP_MODIS caused by input DAO meteorological data are larger at the northern sites than at the southern sites.

GPP calculated using observed meteorological data and smoothed MODIS LAI

Smoothing MODIS LAI can improve the agreement between simulated GPP (GPP_REV2) and GPP_FLUX at all sites. The improvement of GPP_REV2 over GPP_REV1 was moderate at CBS and QYZ and significant at DHS, TMK, and TKY (Fig. 1; Table S1). At DHS, the R^2 values of GPP_REV2 against GPP_FLUX were 0.51 and 0.56 in 2003 and 2004, respectively, significantly higher than the GPP_REV1 values of 0.35 and 0.34. At TMK, the R^2 values of GPP_REV2 reached 0.94, 0.87 and 0.95 in 2001, 2002 and 2003, respectively, while the corresponding values of GPP_REV1 were only 0.69, 0.60 and 0.73. At TKY, the R^2 values of GPP_REV2 were 0.84, 0.81, and 0.80 in 2004, 2005 and 2006, respectively, 0.09, 0.18, and 0.20 higher than the corresponding values of GPP_REV1. The RMSE values of GPP_REV2 were smaller than the corresponding values of GPP_REV1 at all sites.

GPP calculated using observed meteorological data, smoothed MODIS LAI, and calibrated ε_{max}

The calibration of ε_{max} significantly corrects the underestimation of calculated GPP (GPP_REV3) at CBS, QYZ, and TMK. At CBS, the annual means of GPP_REV2 were underestimated by 60.35 and 61.84 % in 2003 and 2004, respectively. These numbers of GPP_REV3 decreased to 21.28 and 20.80 %. At QYZ, the annual means of GPP_REV3 were 20.21 and 19.71 % lower than GPP_FLUX in 2003 and 2004, respectively, while these corresponding values of GPP_REV2 were 46.67 and 46.33 %. At TMK, GPP_REV2 were 38.58–49.73 % lower than GPP_FLUX. The underestimation of GPP_REV3 here ranged from 17.83 to 21.88 %. The RMSE values of GPP_REV3 were obviously lower than the values of GPP_REV2 at CBS, QYZ, DHS, and TMK.

Compared with default ε_{max} used in the MOD17 algorithm, calibrated ε_{max} is significantly higher at CBS, QYZ and TMK and lower at DHS and TKY (Table 2). Calibrated ε_{max} exhibited considerable interannual variations at CBS, DHS, TMK and TKY. At CBS, calibrated ε_{max} was 2.116 g C MJ^{-1} in 2003 and 2.216 g C MJ^{-1} in 2004 while it was only 0.744 g C MJ^{-1} at TKY. The considerable spatial and temporal variations of calibrated ε_{max} indicate that only changes of ε_{max} with land cover types in the MOD17 algorithm are sometimes questionable.

GPP calculated using the sunlit and shaded leaf separation approach

GPP_REV3 still exhibited distinguishable departures from GPP_FLUX (Fig. 1). When GPP_FLUX was high, GPP_REV3 was mostly higher than GPP_FLUX, especially in late spring and summer. In contrast, when GPP_FLUX was low due to low PAR, GPP_REV3 was lower than GPP_FLUX. With GPP (GPP_REV4) calculated using the sunlit and shaded leaf separation approach, these biases were substantially corrected (Fig. 1). GPP_REV4 significantly outperformed GPP_REV3 at all sites.

The R^2 values of GPP_REV4 were above 0.93 at CBS, QYZ, and TMK, ranging from 0.83 to 0.87 at TKY and from 0.51 to 0.52 at DHS (Table S2). Annual mean GPP_REV4 was very close to GPP_FLUX at TMK and TKY and still underestimated by 9.8–17.21 % at the other three sites, but to a lesser degree than GPP_REV3. The RMSE values of GPP_REV4 ranged from 0.88 to 1.24 g C m^{-2} d^{-1}, significantly smaller than the corresponding values of GPP_REV3 at all sits. Calibrated ε_{max_shaded} was significantly higher than ε_{max_sunlit}.

Discussion

The MOD17 algorithm calculates GPP with prescribed ε_{max}, the DAO meteorological data, and the MODIS fPAR product (MOD15A2). The parameters were determined using the BIOME-BGC model. They change only with land cover types and do not vary with space or time (Heinsch et al. 2003). Previous studies indicated that the accuracy of

Table 2 The comparison of ε_{max} used in the MOD 17 algorithm with calibrated ε_{max} at 5 sites in East Asia

Site	Years	Default ε_{max} (g C/MJ)	Calibrated ε_{max} (g C/MJ)	Calibrated ε_{max_sunlit} (g C/MJ)	Calibrated ε_{max_shaded} (g C/MJ)	Site	Years	Default ε_{max} (g C/MJ)	Calibrated ε_{max} (g C/MJ)	Calibrated ε_{max_sunlit} (g C/MJ)	Calibrated ε_{max_shaded} (g C/MJ)
CBS	2003	1.116	2.116	1.000	4.900	TMK	2001	1.103	1.703	0.400	1.500
	2004		2.216	1.100	4.800		2002		1.303	0.400	1.800
QYZ	2003	1.008	1.508	0.800	3.200		2003		1.703	0.400	1.900
	2004		1.508	0.800	3.20	TKY	2004	1.044	0.744	0.800	3.600
DHS	2003	1.259	0.859	0.400	1.700		2005		0.944	0.600	2.900
	2004		0.959	0.400	1.800		2006		0.944	0.800	3.900

GPP calculated using the MOD17 algorithm vary with temporal scales, regions, and land cover types, possibly related to uncertainties in input data and parameterization and also to some limitations of the algorithm (Heinsch et al. 2006; Zhang et al. 2008; Hashimoto et al. 2012). At five forest sites in East Asia, GPP_MODIS showed systematic underestimation, possibly due to insufficient calibration of the key parameter ε_{max} in this region. With observed meteorological data, smoothed LAI, and calibrated ε_{max}, the quality of calculated GPP was significantly improved, indicating the applicably of the MOD17 algorithm in estimating regional GPP in East Asia.

Nevertheless, the departure of GPP_REV3 from tower-based GPP indicates that the MOD17 algorithm can be further refined. Both soil moisture and VPD affect stomata conductance and photosynthesis. Soil moisture can influence GPP even more significantly than VPD because photosynthesis is closely coupled with water supply to the leaves from the soil (Leuning et al. 2005), while VPD represents mostly the degree of atmospheric demand for water. In the MOD17 algorithm, only VPD is used to describe the effect of water supply on photosynthesis. Soil dryness and atmospheric dryness do not always concurrently occur. The stress factor of VPD is unable to represent the impact of soil dryness on photosynthesis. Excluding soil moisture stress factor avoids the requirement for soil moisture simulation and might cause the overestimation of GPP when soil moisture content is extremely low. In monsoon East Asia, the interannual and seasonal variability of precipitation is considerable. Severe seasonal droughts frequently hit the terrestrial ecosystems here, so it is necessary to add a stress factor of soil moisture in the MOD17 algorithm to improve GPP simulation. Several previous studies have incorporated the soil water availability into light use efficiency models based on simulated soil moisture (Potter et al. 1993; Turner et al. 2006) or remotely sensed land surface wetness index (Xiao et al. 2004a, b). The applicability of such algorithms in the MOD17 algorithm needs further exploration.

In the MOD17 algorithm, fPAR is derived from LAI. The errors in LAI will propagate into calculated fPAR and GPP. In southern and coastal areas, abundant cloud contaminations cause remotely sensed LAI to fluctuate unrealistically. Smoothing methods, such as LACC, can effectively remove short fluctuations of remotely sensed LAI but are unable to function well if cloud contamination lasts for several consecutive composite dates. For example, GPP_REV3 and GPP_REV4 were still obviously lower than GPP_FLUX during DOY 50–100 in 2003 and DOY 160–200 in 2004 at DHS, but to a lesser degree than GPP_MODIS, GPP_REV1 and GPP_REV2. During these periods, MODIS LAI was consecutively affected by clouds in this location. In addition, smoothing LAI is unable to correct the systematic bias of remotely sensed LAI. For example, at QYZ, fPAR calculated using smoothed MODIS LAI was systematically lower than the fPAR estimated from PAR observed at the top and bottom of the canopy in the whole year of 2003 and in most times of 2004 (not shown here). The systematical errors of annual GPP caused by the systematic biases of fPAR can be partially offset through tuning ε_{max}. However, this method might result in seasonal discrepancies between measured and simulated GPP. The seasonal bias of MODIS LAI might be the contributor to the obviously faster increases of calculated GPP than GPP_FLUX in spring at TMK and TKY. Improving the retrieval of LAI from remote sensing data and assimilating remotely sensed LAI into the model will further improve GPP calculations using the MOD17 algorithm.

Many studies have demonstrated some vegetation indexes able to effectively estimate GPP and light use efficiency, such as enhanced vegetation index (Hute et al. 2002; Hashimoto et al. 2012) and photochemical reflectance index (Nakaji et al. 2007). Hashimoto et al. (2012) found out that EVI alone was able to track seasonal variations in tower-estimated GPP at 21 globally distributed forest sites while MODIS LAI is the best predictor of annual flux-tower GPP. Xiao et al. (2004a, b) assumed EVI equal to fPAR in the VPM model. This strategy takes advantage of EVI's insensitivity to atmospheric noise and eliminates the need to calculate fPAR from MODIS LAI, which might contain some uncertainties. The applications

of such vegetation indexes in light use efficiency models provide ways to improve GPP calculation data.

Calibrated ε_{max} differs greatly from the default values used in the MOD17 algorithm. It varies significantly in different sites and years. In the MOD17 algorithm, this parameter is assumed to change only with vegetation types. This simplification for this key parameter might prevent the model from correctly reproducing measured GPP at some sites. In this study, this parameter was calibrated with the assumption that the fPAR was correctly calculated. In reality, there are certain uncertainties in fPAR estimated from MODIS LAI. In the future, fPAR should first be correctly calculated. Then ε_{max} can be calibrated and the mechanism underlying the variations of this parameter can be explored. A method to describe the variations of this parameter can then be developed.

The sunlit and shaded leaf separation approach developed here greatly improve GPP simulation due to the proper consideration of different light use efficiency of sunlit and shaded leaves. This new approach alleviated the underestimation of GPP when the sky clearness index was low and the alleviated the overestimation of GPP when the sky clearness index was high (Fig. 2). Under a clear sky, direct PAR accounts for a large fraction of incoming PAR. Sunlit leaves frequently absorb large amounts of PAR above the light saturation point and have low light use efficiency. In contrast, shaded leaves have opportunities to absorb only diffused PAR. Their photosynthesis is normally limited by low PAR and will linearly increase with the increase in APAR, resulting in higher light use efficiency than sunlit leaves. This is confirmed by the different ε_{max} values of sunlit and shaded leaves (Table 2). When the sky clearness index is low, incoming PAR consists mainly of diffused PAR. The fraction of PAR intercepted by shaded leaves, then, will be high. GPP_REV4 will be higher than GPP_REV3 since the ε_{max} value of shaded leaves is higher than the ε_{max} value for the whole canopy (Table 2). When the sky clearness index is high, incoming PAR consists mainly of direct PAR, so the fraction of PAR intercepted by sunlit leaves will be high. GPP_REV4 will then be lower than GPP_REV3 since the ε_{max} value of sunlit leaves is lower than the ε_{max} value for the whole canopy (Table 2). Compared with GPP_REV3, GPP_REV4 showed much smaller biases with changing sky clearness index (Fig. 2).

The proper separation of incoming PAR into the direct and diffused components is important for the calculation of GPP using the sunlit and shaded leaf separation approach. In this study, the empirical algorithm developed by Chen et al. (1999) was directly used to partition direct and diffused PAR. The applicability of this empirical algorithm in East Asia needs further investigation. The new approach improved GPP calculation at different sites and under different conditions of sky clearness. However, it still tends to underestimate GPP when sky clearness index is low and tends to overestimate GPP when sky clearness index is high (Fig. 2), possibly related to its current assumption that ε_{max} does not change with time and intercepted PAR.

Regional GPP of forests over East Asia in 2003 was calculated using the MOD17 algorithm in conjunction with interpolated NCEP meteorological data, smoothed MODIS LAI, and ε_{max} values with and without calibration, and the sunlit and shaded leaf separation approach (Figure S1). The calibration of ε_{max} with tower-based GPP caused total simulated GPP of forests in the study region of East Asia to decrease by 5.5 %, mainly due to a value of calibrated ε_{max} much smaller than the default value used in the MOD17 algorithm for evergreen forests, which account for a large fraction of forests in the study region and have high productivity. Total GPP of forests using the simulated sunlit and shaded leaf separation approach was 9.8 % larger than the value simulated using the MOD17 algorithm. Compared to the MOD17 algorithm, the new approach produced larger GPP in coastal areas and smaller GPP in other areas.

Summary

In this study, tower-based GPP was used to evaluate GPP calculated using the MOD17 algorithm at five forest ecosystems of East Asia. Possible factors causing uncertainties in calculated GPP and potential ways for improving MODIS GPP were analyzed. The following conclusions can be drawn from this study:

(1) GPP_MODIS was systematically underestimated at the CBS, TMK, TKY, and QYZ sites, while it showed random departures from measured GPP at the DHS site. The significant discrepancies between GPP calculated using the MOD17 algorithm and measurements are mainly caused by ε_{max}, followed by fPAR and meteorological data. The default ε_{max} values used in the MOD17 algorithm caused systematic negative biases in calculated GPP at all sites, implying the necessity of calibrating this parameter using tower-based GPP in various ecosystems of East Asia.

(2) With observed meteorological data, fPAR calculated using smoothed LAI, and calibrated ε_{max}, GPP predicted using the MOD17 algorithm, showed satisfying agreement with measured GPP, indicating that the MOD17 GPP algorithm is applicable for calculating GPP of forest ecosystems in East Asia. Calibrated ε_{max} shows considerable variation across different sites and in different years. The development of algorithms to determine this parameter from remote sensing data will definitely further improve the calculation of GPP.

(3) The separation of canopy into sunlit and shaded leaves for individually calculating GPP greatly improved GPP calculation at all five study sites, reducing the

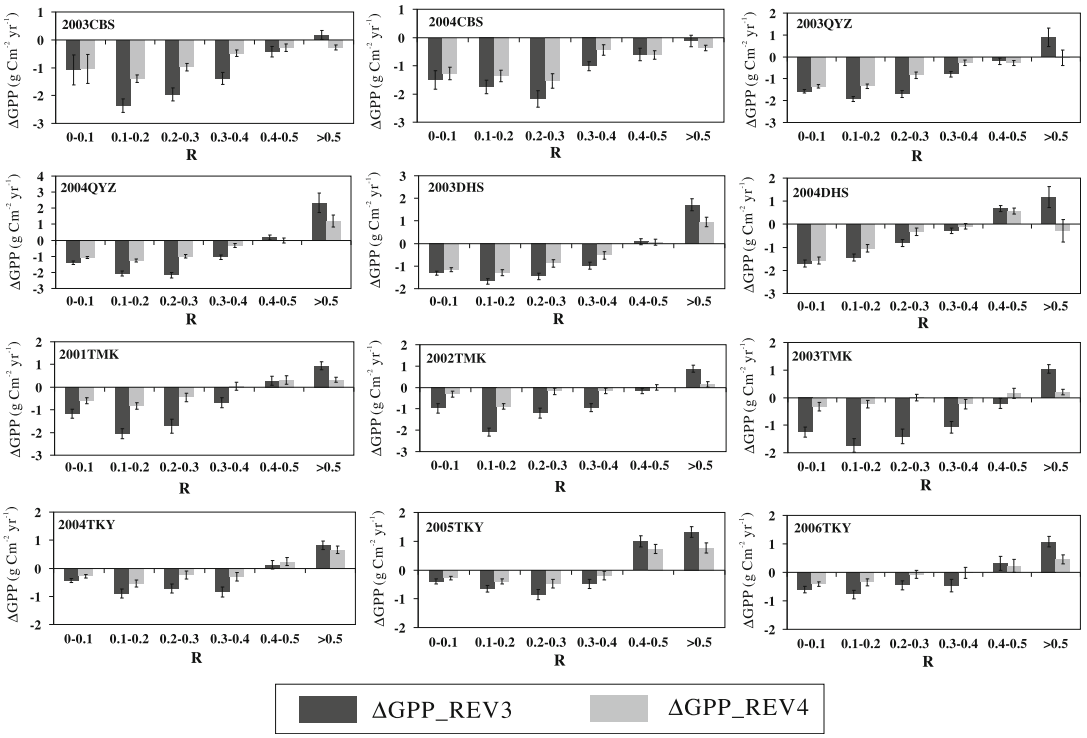

Fig. 2 The average values and the standard errors of ΔGPP = (GPP_FLUX-GPP_MOD4) in each of *R* classes at five sites of East Asia. *R* means the sky clearness index, which equals to PAR/($S_0 \times 0.5 \times \cos\theta$), where S_0 is the solar constant (=1367 W m^{-2}) and θ is the solar zenith angle

overestimation of GPP under clear sky conditions and the underestimation of GPP under cloudy sky conditions. This algorithm keeps the merit of simplicity of the light use efficiency models and captures variations in photosynthetic mechanisms of different leaves responding to APAR. Of course, the applicability and robustness of this algorithm in other areas and ecosystems need further investigation.

Acknowledgments This study was supported by the National Basic Research Program of China (2010CB833503 and 2010CB0705002), the A3 Foresight Program under National Science Foundation of China (30721140307), Doctoral Fund of Ministry of Education of China (20090091110034), the Chinese Academy of Sciences for Strategic Priority Research Program (No. XDA05050602) and the Priority Academic Program Development (PAPD) of Jiangsu Higher Education Institutions. We also greatly thank the ChinaFLUX and AsiaFlux for the provision of flux and meteorological data. We gratefully acknowledge the constructive suggestions by the anonymous reviewers, which helped to improve the quality of manuscript greatly.

References

Baldocchi DD, Falge E, Gu LH, Olson R, Hollinger DY, Running SW, Anthoni P, Bernhofer C, Davis KJ, Evans R, Fuentes J, Goldstein A, Katul G, Law BE, Lee X, Malhi Y, Meyers TP, Munger JW, Oechel WC, Paw UKT, Pilegaard K, Schmid HP, Valentini R, Verma S, Vesala T, Wilson KB, Wofsy SC (2001) FLUXNET: a new tool to study the temporal and spatial variability of ecosystem-scale carbon dioxide, water vapor, and energy flux densities. Bull Am Meteorol Soc 82:2415–2434

Chen JM, Liu J, Cihlar J, Goulden ML (1999) Daily canopy photosynthesis model through temporal and spatial scaling for remote sensing applications. Ecol Model 124:99–119

Chen JM, Deng F, Chen M (2006) Locally adjusted cubic-spline capping for reconstructing seasonal trajectories of a satellite-derived surface parameter. IEEE Trans Geosci Remote Sens 44:2230–2238

De Pury DGG, Farquhar GD (1997) Simple scaling of photosynthesis of leaves to canopies without the errors of big-leaf models. Plant Cell Environ 20:537–557

Fu YL, Yu GR, Sun XM, Li YN, Wen XF, Zhang LM, Li ZQ, Zhao L, Hao YB (2006) Depression of net ecosystem CO_2 exchange in semi-arid *Leymus chinensis steppe* and alpine shrub. Agric For Meteorol 137:234–244

Gu LH, Baldocchi D, Verma SB, Black TA, Vesala T, Falge EM, Dowty PR (2002) Advantages of diffuse radiation for terrestrial ecosystem productivity. J Geophys Res (Atmos) 107:1–23

Hashimoto H, Wang W, Milesi C, White MA, Ganguly S, Gamo M, Hirata R, Myneni RB, Nemani RR (2012) Exploring simple algorithms for estimating gross primary production in forested areas from satellite data. Remote Sens 4:303–326

Heinsch FA, Reeves M, Votava P, Kang S, Milesi C, Zhao M, Glassy J, Jolly WM, Loehman R, Bowker CF, Kimball JS, Nemani RR, Running SW (2003) User's guide: GPP and NPP (MOD17A2/A3) products, NASA MODIS Land Algorithm, Version 2.0. The University of Montana, Missoula, p 57

Heinsch FA, Zhao MS, Running SW, Kimball JS, Nemani RR, Davis KJ, Bolstad PV, Cook BD, Desai AR, Ricciuto DM, Law BE, Oechel WC, Kwon HJ, Luo H, Wofsy SC, Dunn AL, Munger JW, Baldocchi DD, Xu L, Hollinger DY, Richardson AD, Stoy PC, Siqueira MBS, Monson RK, Burns SP, Flanagan LB (2006) Evaluation of remote sensing based terrestrial productivity from

MODIS using regional tower eddy flux network observations. IEEE Trans Geosci Remote Sens 44:1908–1925
Hill MJ, Senarath U, Lee A, Zeppel M, Nightingale JM, Williams RJ, Mavicar TR (2006) Assessment of the MODIS LAI product for Australian ecosystems. Remote Sens Environ 101:495–518
Hirata R, Hirano T, Saigusa N, Fujinuma Y, Inukai K, Kitamoi Y, Takahashi Y, Yamamoto S (2007) Seasonal and international variations in carbon dioxide exchange of a temperate larch forest. Agric For Meteorol 147:110–124
Hute A, Didan K, Miura T, Rodriguez EP, Gao X, Ferreira LG (2002) Overview of the radiometric and biophysical performance of the MODIS vegetation indices. Remote Sens Environ 83:195–213
Kanniah KD, Beringer J, Hutley LB, Tapper NJ, Zhu X (2009) Evaluation of collections 4 and 5 of the MODIS gross primary productivity product and algorithm improvement at a tropical savanna site in northern Australia. Remote Sens Environ 113:1808–1822
Leuning R, Cleugh HA, Zegelin SJ, Hughes D (2005) Carbon and water fluxes over a temperate Eucalyptus forest and a tropical wet/dry savanna in Australia: measurements and comparison with MODIS remote sensing estimates. Agric For Meteorol 129:151–173
Li G, Xin XP, Wang DL, Yang GX, Zhang HB (2008) Estimation of grassland photosynthesis parameters based on MODIS taking Inner Mongolia as an example. Chin J Grassl 30:1–7 (in Chinese)
Metz B, Davidson O, Coninck HD, Loos M, Meyer L (2006) Special report of the intergovernmental panel on climate change. Intergovernmental Panel on Climate Change
Nakaji T, Ide R, Oguma H, Suigusa N, Fujinuma Y (2007) Utility of spectral vegetation index for estimation of gross CO_2 flux under varied sky conditions. Remote Sens Environ 109:274–284
Nightingale JM, Coops NC, Waring RH, Hargrove WW (2007) Comparison of MODIS gross primary production estimates for forests across the USA with those generated by a simple process model, 3-PGS. Remote Sens Environ 109:200–509
Norman JM (1993) Scaling processed between leaf and canopy levels. Scaling physiological processes: leaf to globe. Academic Press, San Diego, pp 41–76
Oliphant AJ, Dragoni D, Deng B, Grimmond CSB, Schmid HP, Scott SL (2011) The role of sky conditions on gross primary production in a mixed deciduous forest. Agric For Meteorol 151:781–791
Potter CS, Randerson JT, Field CB, Matson PA, Vitousek PM, Mooney HA, Klooster SA (1993) Terrestrial ecosystem production: a process model based on global satellite and surface data. Glob Biogeochem Cycles 7:811–841
Running SW, Nemani RR, Heinsch FA, Zhao MS, Reeves M, Hashimoto H (2004) A continuous satellite-derived measure of global terrestrial primary production. Bioscience 54:547–560
Saigusa N, Yamamoto S, Murayama S, Kondo H (2005) Inter-annual variability of carbon budget components in an AsiaFlux forest site estimated by long-term flux measurements. Agric For Meteorol 134:4–16
Sala OE, Jackson RB, Mooney HA, Howarth RW (2000) Methods in ecosystem science. Springer, Berlin
Sun XM, Wen XF, Yu GR, Liu YF, Liu QJ (2006) Seasonal drought effects on carbon sequestration of a mid-subtropical planted forest of southern China. Sci China D Earth Sci 49(Suppl II):110–118
Turner DP, Ritts WD, Cohen WB, Gower ST, Zhao MS, Running SW, Wofsy SC, Urbanski S, Dunn AL, Munger JW (2003) Scaling gross primary production (GPP) over boreal and deciduous forest landscaped in support of MODIS GPP product validation. Remote Sens Environ 88:256–270
Turner DP, Ritts WD, Cohen WB, Maeirsperger TK, Gower ST, Kirschbaum AA, Running SW, Zhao MS, Wofsy SC, Kwon HJ, Meyers TP, Small EE, Kurc SA, Gamon JA (2005) Site-level evaluation of satellite-based global terrestrial GPP and NPP monitoring. Glob Change Biol 11:666–684
Turner DP, Ritts WD, Styles JM, Yang Z, Cohen WB, Law BE, Thornton PE (2006) A diagnostic carbon flux model to monitor the effects of disturbance and interannual variation in climate on regional NEP. Tellus 58B:476–490
Wang YP, Leuning R (1998) A two-leaf model for canopy conductance, photosynthesis and partitioning of available energy I: model description and comparison with multi-layered model. Agric For Meteorol 91:89–111
Xiao XM, Hollinger D, Aber J, Goltz M, Davidson EA, Zhang QY, Moore B III (2004a) Satellite-based modeling of gross primary production in an evergreen needleleaf forest. Remote Sens Environ 89:519–534
Xiao XM, Zhang QY, Braswell B, Urbanski S, Boles S, Wofsy S, Moore B III, Ojima D (2004b) Modelling gross primary production of temperate deciduous broadleaf forest using satellite images and climate data. Remote Sens Environ 91:256–270
Yang FH, Ichii K, White MA, Hashimoto H, Michaelis AR, Votava P, Zhu AX, Huete A, Running SW, Nemani RR (2007) Developing a continental-scale measure of gross primary production by combining MODIS and AmeriFlux data through support vector machine approach. Remote Sens Environ 110:109–122
Yu GR, Wen XF, Sun XM, Tanner BD, Lee XH, Chan JY (2006) Overview of ChinaFLUX and evaluation of its eddy covariance measurement. Agric For Meteorol 137:125–137
Zhang LM, Yu GR, Sun XM, Wen XF, Ren CY, Fu YL, Li QK, Li ZQ, Liu YF, Guan DX, Yan JH (2006a) Seasonal variations of ecosystem apparent quantum yield (α) and maximum photosynthesis rate (P_{max}) of different forest ecosystems in China. Agric For Meteorol 137:176–187
Zhang LM, Yu GR, Sun XM, Wen XF, Ren CY, Song X, Liu YF, Guan DX, Yan JH, Zhang YP (2006b) Seasonal variation of carbon exchange of typical forest ecosystems along the eastern forest transect in China. Sci China Earth Sci 49:47–62
Zhang YQ, Yu Q, Jiang J, Tang YH (2008) Calibration of Terra/MODIS gross primary production over an irrigated cropland on the North China Plain and an alpine meadow on the Tibetan Plateau. Glob Change Biol 14:757–767
Zhang FM, Ju WM, Shen SH, Wang SQ, Yu GR, Han SJ (2012) Variations of terrestrial net primary productivity in East Asia. Terr Atmos Ocean Sci. doi:10.3319/TAO.2012.03.28.01(A)
Zhao MS, Running SW (2006) Sensitivity of Moderate Resolution Imaging Spectroradiometer (MODIS) terrestrial primary production to the accuracy of meteorological reanalyses. J Geophys Res 111:1002–1015
Zhao MS, Heinsch FA, Nemani RR, Running SW (2005) Improvements of the MODIS terrestrial gross and net primary production global data set. Remote Sens Environ 95:164–176